Desalination and Water Treatment
www.deswater.com

doi: 10.1080/19443994.2014.992976

57 (2016) 4671–4680
February

Taylor & Francis
Taylor & Francis Group

Performance and mechanism study on phosphate adsorption onto activated carbon fiber loading lanthanum and iron oxides

Ling Zhang, Mengxue Li, Yan Gao, Jianyong Liu*, Yunfeng Xu

School of Environmental and Chemical Engineering, Shanghai University, 333 Nanchen Road, Shanghai 200444, P.R. China, Tel. +86 21 6613 7793; Fax: +86 21 66137725; emails: zhanglinglzu@staff.shu.edu.cn (L. Zhang), limengxue@shu.edu.cn (M. Li), 740937899@shu.edu.cn (Y. Gao), Tel. +86 21 6613 7769; Fax: +86 21 66137761; emails: liujianyong@shu.edu.cn (J. Liu), yfxu@shu.edu.cn (Y. Xu)

Received 20 May 2014; Accepted 23 November 2014

ABSTRACT

A hybrid sorbent of lanthanum and iron oxides doped onto activated carbon fiber (ACF–LaFeO) was developed for the removal of phosphate from water. The effects of *n* (La)/*n* (Fe), total metal ion concentration, activation time, and activation temperature on the sorbent performance were studied by single-factor method. Response surface method (RSM), based on three-variable, three-level Box–Behnken design (BBD), was used to optimize the preparation parameters. The phosphate adsorption mechanism was investigated by Brunauer–Emmett–Teller (BET) analysis, Fourier transform infrared (FT–IR) spectroscopy analysis, and the test of adsorption amount dependence on the solution pH. The possible adsorption mechanisms could be a combination of electrostatic interaction, ion exchange, and Lewis acid–base interactions, depending on solution pH.

Keywords: Phosphate adsorption; Lanthanum iron oxides (LaFeO); Activated carbon fiber (ACF); Response surface method (RSM); Mechanism

1. Introduction

Eutrophication is posing a great threat to the safety of drinking water quality [1–3]. Control of phosphorus has the highest priority because of its presumed leading role in limiting development of aquatic plant biomass [4]. Therefore, phosphorus removal from wastewater has been considered to be the key strategy [5]. Methods of phosphorus removal mainly include: chemical phosphorus removal [6], biological phosphorus removal, [7,8] and adsorption [9]. Among them, adsorption is effective, environment-friendly and low-cost, but with the main challenge of finding materials with high adsorption capacity. Conventional adsorbents involve activated alumina [10–12], activated carbon [13,14], iron (hydr) oxides [15–17], zeolite, [18,19] and low-cost clay [20–22].

Recently, metal ions including aluminum, iron, titanium, zirconium, and manganese especially rare earth elements such as lanthanum are known to have a specific affinity for fluoride, arsenic, and phosphates. Lanthanum with nontoxic and environment-friendly properties [23] has been extensively developed as the adsorbents for phosphate anions from aqueous solutions and has shown promising results [24–26], but the high price and scarcity of the lanthanum resources hinder its practical applications. In the past decades, ferric (hydr) oxides have been found to possess ability

*Corresponding author.

to anionic pollutants [17,27,28] with cheap price and sufficient resources. Mixing lanthanum with ferric would be a possible economic way to reduce the dosage of rare earth metals, and to maintain high phosphate adsorption capacity at the same time.

Activated carbon fiber (ACF) has been proved to be a cheap and easily available substrate, with high adsorption capacity [29], huge BET surface area [30], micropores of great pore volume [31], and more importantly the ease of recovery. In our previous study, lanthanum iron hydroxide-doped ACF (ACF–LaFeOH) has been successfully prepared by a modified form of a proprietary synthetic process developed by SolmeteX, with a simple process of loading a variety of metals at the same time [32]. But the stability of ACF–LaFeOH was not so good because the binding affinity between ACF and lanthanum iron hydroxides (LaFeOH) is relative weak. For this problem, it could be a good selection to load LaFeO onto ACF by a typical method comprising immersion-filter-drying-calcination-screening [33].

The objectives of this study were: (1) to optimize the preparation conditions of ACF–LaFeO using single-factor and response surface methodologies (RSM); (2) to investigate the phosphate removal performance of the sorbent; and (3) to study the adsorption mechanism by Brunauer–Emmett–Teller (BET) analysis, Fourier transform infrared (FT–IR) spectroscopy analysis, and the test of adsorption amount dependence on the solution pH.

2. Materials and methods

2.1. Materials

ACF was gained from Qinhuangdao Zichuan Carbon Fiber Co. Ltd (China). The specific surface and mean pore size of ACF is 1,326-m^2/g, 1.8-nm, respectively. Potassium dihydrogen phosphate, lanthanum nitrate, ferric nitrate, ascorbic acid, and molybdenum acid ammonium were purchased from Sinopharm Chemical Reagent Co. Ltd. (China). All the chemical reagents used were of analytical grade.

2.2. Preparation and characterization of the sorbents

ACF was fully washed several times with deionized water and cut to the square block of 0.4–0.6 cm. At this time, it was introduced to solutions containing lanthanum nitrate and iron nitrate with different impregnation mole ratios (n (La)/n (Fe), %) for modification treatment. After filtration, the modified ACF was dried overnight at 105˚C and then calcined, sealed with a tin foil at different temperatures in an oven for various time periods. Finally, ACF–LaFeO was sealed and reserved for further experiments.

BET surface area (S_{BET}) measurements were performed on a QUADRASORB SI instrument (Quantachrome Co. Ltd, USA). Nitrogen adsorption was carried out at −196.15˚C. FT–IR measurements were performed on a Nicolet FT–IR 380 instrument (Thermo Scientific Co. Ltd., USA). The spectrum of dry potassium bromide was taken for background subtraction. Each spectrum was obtained by accumulating 152 scans in transmission.

2.3. Adsorption tests and analytical methods

A phosphate stock solution used for the experiments was prepared by dissolving an accurately weighed sample of anhydrous potassium dihydrogen phosphate (KH_2PO_4 purchased from Merck) in deionized water.

ACF–LaFeO (0.04-g) was added into a 50-mL conical flask filled with 40-mL (1-g/L dosage) of phosphate solution (20-mg P/L). The solutions were stirred on a shaker bath at 120-rpm for 24 h at room temperature. After the contact time, the solution was removed by filtering through a syringe nylon-membrane filter (pore size 0.45-μm; Shanghai Minglie Science Technology Co. Ltd). Then, the solution was used to determine the phosphate concentration by the molybdenum antimony method (Model 721, Shanghai Metash Instruments Co. Ltd, China) at λ_{max} of 700-nm with the blank sample containing only deionized water as a reference solution [34]. In order to reduce the experimental errors, all experiments were conducted two times and the mean experimental data were recorded.

The removal efficiency (E, %) and the adsorption capability (Q, mg/g) of phosphate on ACF–LaFeO were calculated from Eq. (1):

$$E = (C_i - C_e)/C_i \times 100 \qquad q = (C_i - C_e)\, V/m \tag{1}$$

where V is the volume of phosphate solution in L, m is the sorbent mass in g, and C_i and C_e are the initial and equilibrium phosphate concentrations in mg P/L, respectively.

2.4. RSM experimental design

Box–Behnken experimental design, which is a widely used form of RSM [35], was applied for the optimization of ACF–LaFeO preparation conditions, using the design expert statistical software (version 7.1.6, STAT-EASE Inc., Minneapolis, MN, USA).

After using multiple quadratic equations to fit response value, n (La)/n (Fe) (X_1, %), total metal ion concentration (X_2, mol/L), and activation time (X_3, min) had a great effect on the removal rate of phosphate [36]. The validity of the model was expressed in terms of the coefficient of determination R^2, and the adequacy of the model was further evaluated by analysis of variance (ANOVA).

For statistical calculation, the variables X_i is encoded as x_i according to Eq. (2):

$$x_i = (X_i - X_0)/\Delta X \tag{2}$$

where X_0 is the value of X_i at the center point and ΔX represents the step change.

The quadratic equation model for predicting the target function can use formula (3):

$$Y = b_0 + \sum_{i=1}^{k} b_i x_i + \sum_{i=1}^{k} b_{ii} x_i^2 + \sum_{i=1}^{k-1} \sum_{j=i+1}^{k} b_{ij} x_i x_j \tag{3}$$

where Y is the predicted response value (the removal rate of phosphate); b_0 is the constant coefficient; b_i is the linear coefficients; b_{ii} is the quadratic coefficients; b_{ij} is the interaction coefficients; and x_i and x_j are the coded levels of process factors studied.

3. Results and discussion

3.1. The effect of different factors on ACF–LaFeO preparation

The preparation conditions of ACF–LaFeO were studied by single-factor method. The concentration of phosphate was 20-mg P/L, the dosage of absorbent was 1.0-g/L, and the adsorption time was 24 h. The results are illustrated in Fig. 1.

It can be found in Fig. 1(a) that the phosphate removal efficiency decreased with the decrease of n (La)/n (Fe). This is because lanthanum had higher phosphate adsorption capacity than iron. Higher lanthanum content of the sorbent makes better phosphorus removal effect.

From Fig. 1(b) we can find that phosphate removal efficiency first increased with increasing phosphate concentration and then decreased after the concentration came to 0.15-mol/L. This is possibly because, the adsorption sites were enough to load metal oxides on ACF when phosphate concentration was lower than 0.15-mol/L. While with higher phosphate concentration, there were no adsorption sites to load metal oxides and there were considerable self-agglomerates caused by loading too many metal oxides,which led to saturation of the sorbent sites.

It can be observed in Fig. 1(c) that phosphate removal efficiency increased at first sharply and then decreased with an increase of the activation time. This suggests that, it requires enough time for lanthanum and ferric nitrate to convert into LaFeO. But a continued increase of the activation time made the microspore size of ACF to decrease, which reduced the active sites of reaction with the phosphate ions.

Fig. 1(d) points out that removal efficiency increased with the rise of activation temperature. This owes to the fact that the LaFeO has distinct oxide forms at different activation temperatures, which are likely to have different affinities to phosphate.

3.2. Response surface methodology

3.2.1. The variable and value of RSM

According to Fig. 1, the phosphate removal efficiency ranged from 21.2 to 64.2% for n (La)/n (Fe), from 32.3 to 58.7% for solution concentration, from 56.4 to 73.1% for activation time, and from 50.6 to 60.3% for activation temperature, respectively. It is found that the effect of activation temperature on phosphate removal changed in a small range. Therefore, n (La)/n (Fe) (%), solution concentration (mol/L), and activation time (min) were chosen as the main factors which affect effectively phosphate removal. As presented in Table 1, the levels of independent factors of the experimental design were chosen based on the single-factor experiment. The data (the removal efficiency of phosphate, the content of Fe, solution concentration, and activation time) based on the matrix experimental design are tabulated in Table 2.

3.2.2. Regression model equation

From Table 2, phosphate removal efficiency was between 30.2 and 68.2%, when the dosage of the sorbent and the phosphate concentration were 1.0-g/L and 20-mg P/L. The groups of 13–17 as mean values were mainly to measure experimental errors.

The regression model equation explains the relationship between phosphate removal efficiency (y) with each factor code value, which is shown in the following:

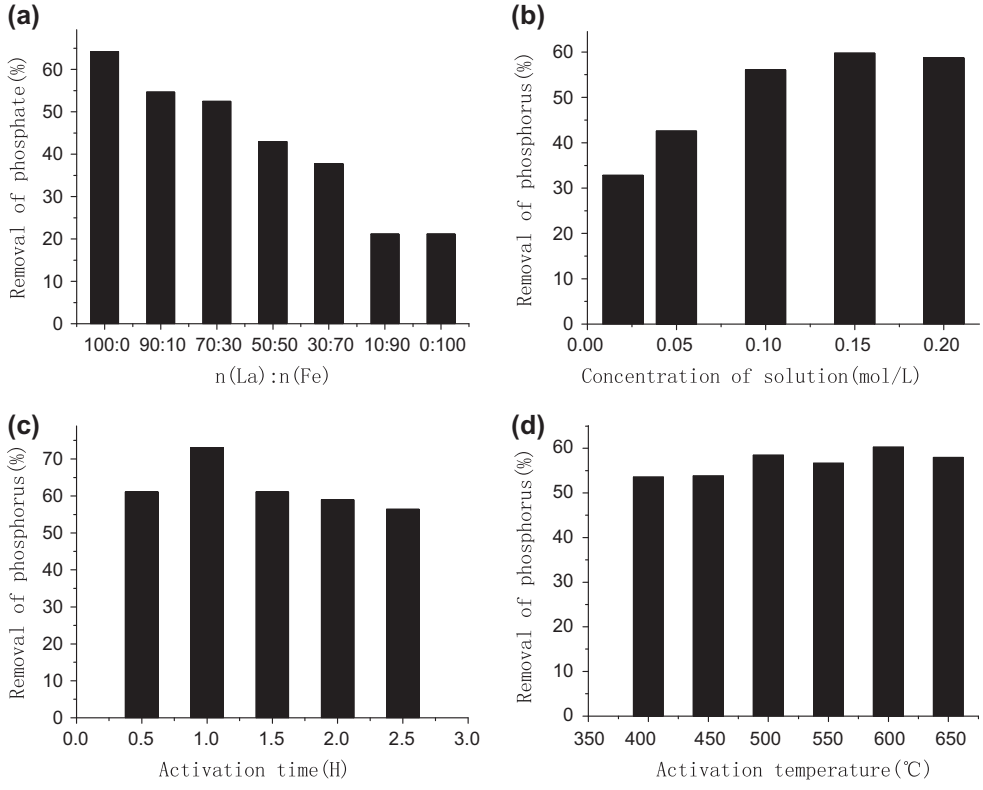

Fig. 1. The effects of different variables on the removal efficiency: (a) solution concentration = 0.1-mol/L, activation time = 2.0 h, and activation temperature = 650℃; (b) n (La)/n (Fe) = 70:30, activation time = 2.0 h, and activation temperature = 650℃; (c) solution concentration = 0.15-mol/L, n (La)/n (Fe) = 70:30, and activation temperature = 650℃; (d) solution concentration = 0.15-mol/L, n (La)/n (Fe) = 70:30, and activation time = 1.5 h. Initial phosphate concentration of 20-mg P/L, sorbent dosage 1.0-g/L, and temperature = 20 ± 0.5℃.

Table 1
Experimental ranges and levels of the independent test variables

Variables	Units	Real values of coded levels		
		−1	0	1
The content of ferrum	%	0	25.0	50.0
Solution concentration	mol/L	0.05	0.13	0.20
Activation time	min	30.0	60.0	90.0

$$y = -2.53787 + 389.88797\ x_1 - 0.19393\ x_2 + 0.95413x_3 + 0.54774x_1x_2 - 0.96996x_1x_3 - 4.10802E-003x_2x_3 - 885.14732{x_1}^2 + 4.43731E-005{x_2}^2 - 4.96161E-003{x_3}^2$$

3.2.3. ANOVA analysis

The results of the quadratic model in the form of analysis of variance (ANOVA) for phosphate removal efficiency are shown in Table 3. In general, the value of sum of squares could be used to measure the significant variables in the model; the higher value of sum of squares indicated it was more remarkable in statistics. According to Table 3, the sum of square was 693.0 for the content of ferrum, 683.5 for the solution concentration, and 130.8 for the activation time, which indicated that content of ferrum and solution concentration had a greater effect than the activation time on the phosphate removal. In addition, it was known that the corresponding variables would be more significant if the p-value was smaller than 0.05. So the model of x_1, x_2, x_3, x_1x_3, x_2x_3, ${x_1}^2$, ${x_3}^2$, except ${x_2}^2$ and x_1x_2 were significant and conformed to the standard. The F values in Table 3 for most of the regression were high, which showed that the regression model could fit

Table 2
Experimental design matrix and results

Run	Sorbent preparation variables			The removal efficiency of phosphate (%)
	The content of ferrum	Solution concentration	Activation time	
	(x_1)	(x_2)	(x_3)	
1	0	0.05	60.0	49.74
2	0	0.20	60.0	68.23
3	50.0	0.05	60.0	30.23
4	50.0	0.20	60.0	52.82
5	25.0	0.05	30.0	30.74
6	25.0	0.20	30.0	51.80
7	25.0	0.05	90.0	44.10
8	25.0	0.20	90.0	56.42
9	0	0.13	30.0	53.85
10	50.0	0.13	30.0	40.50
11	0	0.13	90.0	67.20
12	50.0	0.13	90.0	41.53
13	25.0	0.13	60.0	54.28
14	25.0	0.13	60.0	54.07
15	25.0	0.13	60.0	56.42
16	25.0	0.13	60.0	54.37
17	25.0	0.13	60.0	55.91

Table 3
Analysis of variance (ANOVA) for response surface quadratic model for phosphate removal

Source	Sum of square	DF	Mean square	*F*-value	*p*-value
Model	1,768.32	9	196.48	93.70	<0.0001
x_1	693.00	1	693.00	330.50	<0.0001
x_2	683.47	1	683.47	325.95	<0.0001
x_3	130.82	1	130.82	62.39	<0.0001
x_1x_2	4.22	1	4.22	2.01	0.1990
x_1x_3	19.05	1	19.05	9.09	0.0195
x_2x_3	37.97	1	37.97	18.11	0.0038
x_1^2	104.38	1	104.38	49.78	0.0002
x_2^2	3.238E-003	1	3.238E-003	1.544E-003	0.9697
x_3^2	83.96	1	83.96	40.04	0.0004
Residual	14.68	7	2.10		
Lack of fit	11.14	3	3.71	4.20	0.0997
Pure error	3.54	4	0.88		
Cor total	1,783.00	16			

Note: R^2, R^2_{adj} (coefficient of determination) of the model is 0.9918 and 0.9812.

well. The *F* value of 93.7 showed that the model could fit well between the variables and the corresponding value of the function. The fitting degree of regression equation could be determined by correlation coefficient model. The R^2 and R^2_{adj} values of regression equation were 0.9918 and 0.9812, respectively, by which the relationship between phosphate removal efficiency and the preparation factors could be effectively predicted.

From Fig. 2(c), the experiment data distributed near the straight line. It showed that the model could be used to analyze and predict the relationship between the parameters and the effect of phosphate removal.

Three-dimensional (3D) response surfaces (Fig. 2(a) and (b)) demonstrated that there was an interaction effect among the three factors. The curve plots showed that ACF–LaFeO successfully removed phosphate.

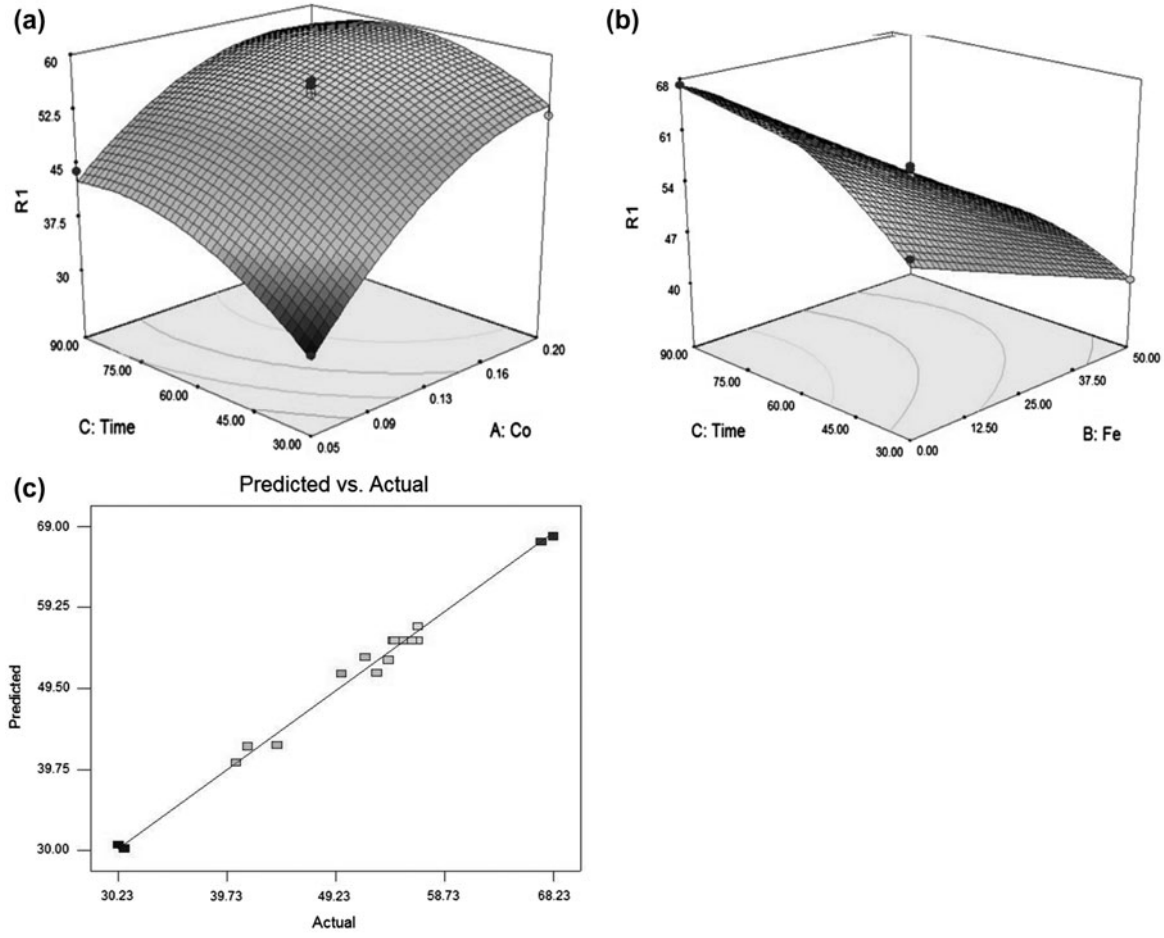

Fig. 2. The three-dimensional response plot of the effects of (a) activation time and solution concentration, n (La)/n (Fe) = 75:25; (b) activation time and n (La)/n (Fe), solution concentration = 0.13-mol/L, and (c) the plot of predicted value versus actual values for removal efficiency.

Based on Fig. 2, interaction effects between solution concentration and activation time, as well as between activation time and n (La)/n (Fe), could be read out.

3.2.4. Model adequacy checking and optimal conditions

The optimal preparation conditions were illustrated: n (Fe)/n (La) of 2.4:97.6%, total concentration of 0.17-mol/L, and activation time of 70.3 min. Phosphate removal efficiency of the sorbent ACF–LaFeO at the optimal preparation conditions reached 68.3%, which indicated that the performance of the novel sorbent was satisfactory. In order to verify the model, three experimental conditions for the preparation of ACF–LaFeO were investigated as shown in Table 4. We also compared the predicted and experimental values for phosphate removal efficiency, as shown in Fig. 3. It indicated that the predicted values and the experimental results are in good coherence.

4. Sorbent characterization and adsorption mechanism study

4.1. Sorbent characterization

4.1.1. BET analysis

The specific surface area, pore size, and pore volume of ACF and ACF–LaFeO are shown in Table 5. It was clear that the surface area of ACF–LaFeO was reduced rapidly compared to ACF, and the pore size and pore volume had a greater increase. That is attributed to the developed internal pores of ACF, which influenced the specific surface area, pore size, and pore volume. The surface of ACF–LaFeO was covered

Table 4
The experimental conditions for model validation

Run	The content of ferrum (%)	The solution concentration (mol/L)	Activation time (min)
1	2.4	0.2	70.3
2	3.0	0.2	77.9
3	0.3	0.1	87.0

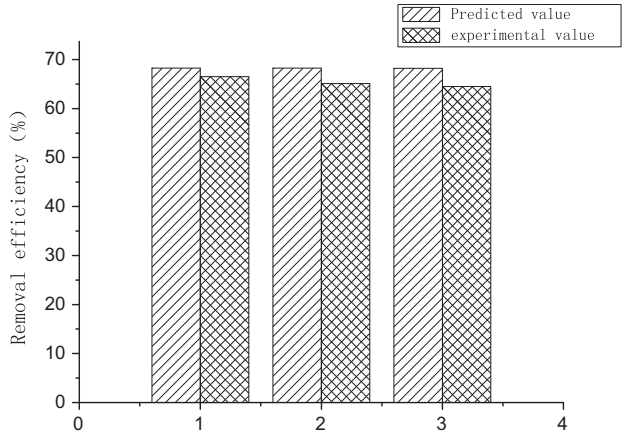

Fig. 3. The predicted value and experimental value for model validation. Initial phosphate concentration of 20-mg P/L, sorbent dosage 1.0-g/L, and temperature = 20 ± 0.5℃.

with a layer of granular active metal oxides which blocked the pores. The reduced parameter value might be due to the granular active metal oxides preventing N_2 to contact the internal pores in the measurement process. At the same time, pore size and pore volume of sorbent ACF–LaFeO were larger than those of ACF, which might be due to the metal particles in the porous material's internal crystallization. For the composite sorbent, most of the specific surface area was covered by metal particles on the outer layer. Surface area of composite sorbent was less than ACF, but still could provide a premise for better adsorption properties. Physical change of ACF–LaFeO also showed that metal particles loaded successfully on ACF.

4.1.2. FT–IR analysis

FT–IR spectra of ACF, ACF–LaFeO as well as, ACF–LaFeO after phosphate adsorption are presented in Fig. 4(a)–(c). By comparing Fig. 4(b) with Fig. 4 (a), new peaks at –588 and –521-cm^{-1} were found representing the characteristic frequency of La–O and Fe–O vibration, indicating that lanthanum and ferric were indeed loaded onto the surface of ACF. Fig. 4(c) indicates the frequency of La–O and Fe–O vibration moved to –569 and preparation conditions –512-cm^{-1} after phosphate adsorption, due to the fact that the active La and Fe sites reacted with phosphate. In Fig. 4(c), the band at preparation conditions –947-cm^{-1} was attributed to the bend vibration of O–P–O and a new peak at –419-cm^{-1} was attributed to La–O coordination between the active La sites and the oxygen anion in the phosphate.

4.2. Effect of solution pH on the adsorption

The phosphate adsorption onto ACF–LaFeO was tested at various pH values ranging from 2.0 to 12.0 under the experimental conditions: initial phosphate concentration of 20-mg P/L, sorbent dosage of 1.0-g/L, and temperature of 20 ± 0.5 ℃. The effect of pH on adsorption capacity was also investigated and it is depicted in Fig. 5. It can be obviously found that the phosphate adsorption on ACF–LaFeO was strongly dependent on the pH value. The adsorption capacity of ACF–LaFeO increased with increasing pH from 2.0 to 4.0 at first and then decreased slowly till pH 8.0, then significantly decreased from 8.0 to 12.0. The sorbent showed a considerably high adsorption capacity over a relatively wide pH range of 4.0–8.0 and the

Table 5
Specific surface area, pore size, and pore volume of ACF and composite sorbent ACF–LaFeO

Samples	S_{BET} (m^2/g)	Pore size (nm)	Pore volume (cm^3/g)
ACF	1326.07	1.81	0.22
ACF–LaFeO	734.14	1.94	0.26

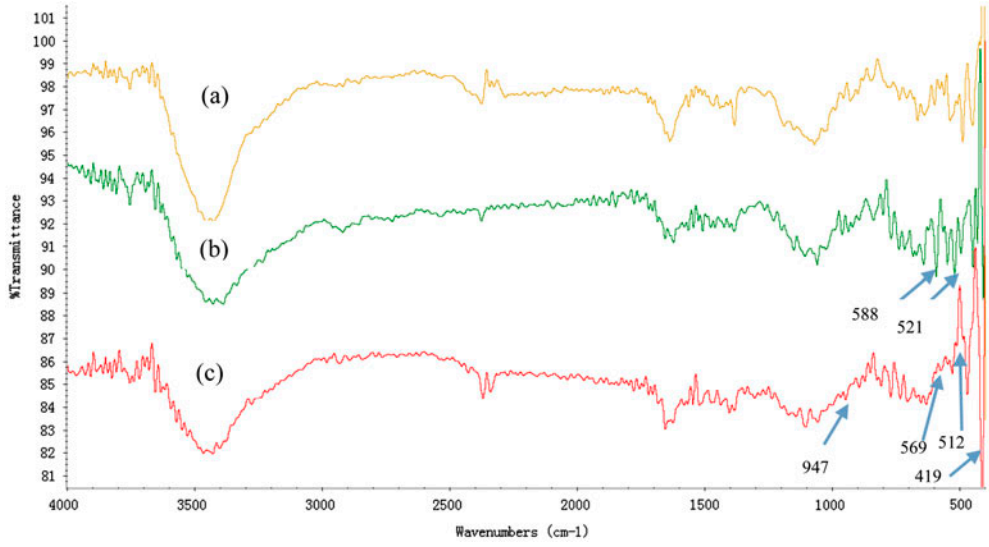

Fig. 4. The FT–IR spectra of (a) ACF, (b) ACF–LaFeO, and (c) ACF–LaFeOP.

pH_{ZPC} of the sorbent was 9.4. In our previous study [32], the optimum pH for phosphate adsorption onto ACF–LaFeOH (with pH_{ZPC} of 8.5) was as low as 4.0. It was clear that the pH_{ZPC} increased with doping LaFeO onto ACF and the relatively high optimum adsorption pH range was related to the higher pH_{ZPC}.

Based on the pKa values for phosphate reported in the literature, the species of phosphorus is different at different pH, as shown in the following:

$$H_3PO_4 \overset{K_1}{\leftrightarrow} H_2PO_4^- + H^+ \overset{K_2}{\leftrightarrow} HPO_4^{2-} + 2H^+ \overset{K_3}{\leftrightarrow} PO_4^{3-} + 3H^+$$

where $pK_1 = 2.15$, $pK_2 = 7.20$, and $pK_3 = 12.33$, respectively [37].

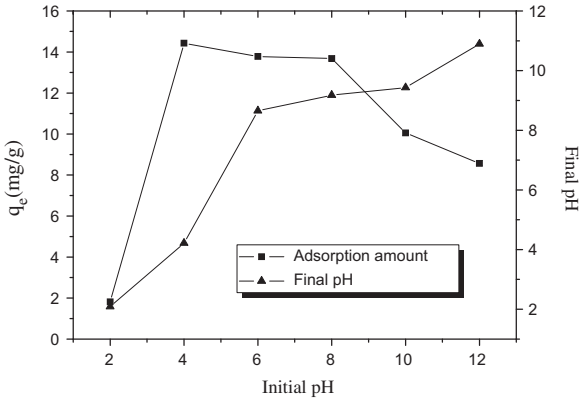

Fig. 5. Effect of solution pH on phosphate adsorption phosphate. Initial phosphate concentration of 20-mg P/L, sorbent dosage 1.0-g/L, and temperature = 20 ± 0.5°C.

When the pH value is about 2.0, the predominant species of phosphorus exists mainly in the form of H_3PO_4. When the pH is in the range of 2.0–12.0, $H_2PO_4^-$ and HPO_4^{2-} are the dominant species. Under very alkaline conditions, PO_4^{3-} is more prevalent.

When the pH value is lower than 2.13, the predominant species of phosphate is the neutral H_3PO_4, which is weakly attached to the sites of ACF–LaFeO. However, $La^{3+}$and Fe^{3+} may leach out from ACF–LaFeO at low pH 2–4 [38,39].

At pH <9.4, the functional groups in the surface of sorbents are protonated and favor the approach of $H_2PO_4^-$ and HPO_4^{2-} as the result of electrostatic forces. It is also revealed that the pH values of solution increases, indicating that phosphate adsorption onto ACF–LaFeO is also the result of ligand exchange between phosphate and hydroxide groups loaded on the sorbent.

As the pH > 9.4, the degree of protonation decreases, and the functional groups become negatively charged which cannot benefit for the phosphate adsorption. At the same time, the values of the concentration of hydroxyl ions are high and the low phosphate uptake in alkaline pH range can also be attributed to competition between hydroxide ions and phosphate ions for adsorption sites. Consequently, electrostatic repulsive forces are operative, and the ion exchange is weakened. Hence, it is likely that Lewis acid–base interaction mechanism that the metal active site reacts with oxygen anion in the phosphate governed due to the existing amount of phosphate adsorption.

Through the above analysis, the main adsorption mechanism could be a combination of electrostatic interaction, ion exchange, and Lewis acid–base interactions, depending on solution pH.

5. Conclusion

The novel sorbent ACF–LaFeO was successfully prepared by loading LaFeO onto ACF, which was confirmed based on the results of BET analysis and FT–IR analysis. The sorbent could achieve phosphate removal of 68.3% under the optimum preparation conditions (n (La)/n (Fe)(%) of 2.4%:97.6%, solution concentration of 0.17-mol/L, and activation time of 70.3 min, respectively) obtained from RSM design method. The effective phosphorus removal rate demonstrated that ACF–LaFeO can be used for phosphate removal from water. The pH_{ZPC} of ACF–LaFeO is 9.4, obviously higher than that of ACF–LaFeOH which was prepared in our previous study. The higher pH_{ZPC} led to the relatively wider optimum adsorption pH range in removing phosphate from water. The mechanistic consideration was also discussed, which illustrated that phosphate reacted with ACF–LaFeO by means of electrostatic interaction, ion exchange, and Lewis acid–base interactions.

Acknowledgments

The work was supported by National Natural Science Foundation of China (21207085, 41472312), Innovation Program of Shanghai Municipal Education Commission (14YZ014) and Program for Innovative Research Team in University (IRT13078).

Abbreviations

ACF	activated carbon fiber
ACF–LaFeOH	lanthanum iron hydroxides doped onto activated carbon fiber [32]
ACF–LaFeO	lanthanum and iron oxides doped onto activated carbon fiber
LaFeOH	lanthanum iron hydroxides
LaFeO	lanthanum and iron oxides
RSM	response surface method
BBD	three-variable, three-level Box–Behnken design
BET	Brunauer–Emmett–Teller
FT–IR	Fourier transform infrared

References

[1] S.K. Ramasahayam, L. Guzman, G. Gunawan, T. Viswanathan, A Comprehensive review of phosphorus removal technologies and processes, J. Macromol. Sci. Part A 51 (2014) 538–545.

[2] P. Loganathan, S. Vigneswaran, J. Kandasamy, N.S. Bolan, Removal and recovery of phosphate from water using sorption, Crit. Rev. Env. Sci. Technol. 44 (2014) 847–907.

[3] B.E. Rittmann, B. Mayer, P. Westerhoff, M. Edwards, Capturing the lost phosphorus, Chemosphere 84 (2011) 846–853.

[4] W.M. Lewis, W.A. Wurtsbaugh, H.W. Paerl, Rationale for control of anthropogenic nitrogen and phosphorus to reduce eutrophication of inland waters, Environ. Sci. Technol. 45 (2011) 10300–10305.

[5] A. Guzzon, A. Bohn, M. Diociaiuti, P. Albertano, Cultured phototrophic biofilms for phosphorus removal in wastewater treatment, Water Res. 42 (2008) 4357–4367.

[6] Y. Zhou, X.-H. Xing, Z. Liu, L. Cui, A. Yu, Q. Feng, H. Yang, Enhanced coagulation of ferric chloride aided by tannic acid for phosphorus removal from wastewater, Chemosphere 72 (2008) 290–298.

[7] A. Broughton, S. Pratt, A. Shilton, Enhanced biological phosphorus removal for high-strength wastewater with a low rbCOD: P ratio, Bioresour. Technol. 99 (2008) 1236–1241.

[8] Y.G. Chen, A.A. Randall, T. McCue, The efficiency of enhanced biological phosphorus removal from real wastewater affected by different ratios of acetic to propionic acid, Water Res. 38 (2004) 27–36.

[9] I. Perassi, L. Borgnino, Adsorption and surface precipitation of phosphate onto $CaCO_3$–montmorillonite: Effect of pH, ionic strength and competition with humic acid, Geoderma 232–234 (2014) 600–608.

[10] O.K. Borggaard, B. Raben-Lange, A.L. Gimsing, B.W. Strobel, Influence of humic substances on phosphate adsorption by aluminium and iron oxides, Geoderma 127 (2005) 270–279.

[11] E.W. Shin, J.S. Han, M. Jang, S.H. Min, J.K. Park, R.M. Rowell, Phosphate adsorption on aluminum-impregnated mesoporous silicates: Surface structure and behavior of adsorbents, Environ. Sci. Technol. 38 (2004) 912–917.

[12] A. Sousa, T. Braga, E.C. ChagasGomes, A. Valentini, E. Longhinotti, Adsorption of phosphate using mesoporous spheres containing iron and aluminum oxide, Chem. Eng. J. 210 (2012) 143–149.

[13] M. Srimurali, A. Pragathi, J. Karthikeyan, A study on removal of fluorides from drinking water by adsorption onto low-cost materials, Environ. Pollut. 99 (1998) 285–289.

[14] D. Mohan, C.U. Pittman Jr., Arsenic removal from water/wastewater using adsorbents—A critical review, J. Hazard. Mater. 142 (2007) 1–53.

[15] S.H. Lin, H.C. Kao, C.H. Cheng, R.S. Juang, An EXFAS study of the structures of copper and phosphate sorbed onto goethite, Colloids Surf., A 234 (2004) 71–75.

[16] R.S. Juang, J.Y. Chung, Equilibrium sorption of heavy metals and phosphate from single- and binary-sorbate solutions on goethite, J. Colloid Interface Sci. 275 (2004) 53–60.

[17] J. Ren, N. Li, L. Zhao, N. Ren, Enhanced adsorption of phosphate by loading nanosized ferric oxyhydroxide on anion resin, Front. Environ. Sci. Eng. 8 (2014) 531–538.

[18] M. Zamparas, M. Drosos, Y. Georgiou, Y. Deligiannakis, I. Zacharias, A novel bentonite-humic acid composite material Bephos™ for removal of phosphate and ammonium from eutrophic waters, Chem. Eng. J. 225 (2013) 43–51.
[19] M. Gibbs, D. Özkundakci, Effects of a modified zeolite on P and N processes and fluxes across the lake sediment-water interface using core incubations, Hydrobiologia 661 (2011) 21–35.
[20] N. Yaghi, H. Hartikainen, Enhancement of phosphorus sorption onto light expanded clay aggregates by means of aluminum and iron oxide coatings, Chemosphere 93 (2013) 1879–1886.
[21] M.P.F. Fontes, S.B. Weed, Phosphate adsorption by clays from Brazilian Oxisols, relationships with specific surface area and mineralogy, Geoderma 72 (1996) 37–51.
[22] A. Violante, M. Pigna, Competitive sorption of arsenate and phosphate on different clay minerals and soils, Soil Sci. Soc. Am. J. 66 (2002) 1788–1796.
[23] S.A. Wasay, J. Haran, S. Tokunaga, Adsorption of fluoride, phosphate, and arsenate ions on lanthanum impregnated silica gel, Water Environ. Res. 68 (1996) 295–300.
[24] O. Encai, Z. Junjie, M. Shaochun, W. Jiaqiang, X. Fei, M. Liang, Highly efficient removal of phosphate by lanthanum-doped mesoporous SiO_2, Colloid Surf. A 308 (2007) 47–53.
[25] P. Ning, H.-J. Bart, B. Li, X. Lu, Y. Zhang, Phosphate removal from wastewater by model-La(III) zeolite adsorbents, J. Environ. Sci. 20 (2008) 670–674.
[26] F. Haghseresht, S. Wang, D.D. Do, A novel lanthanum-modified bentonite, Phoslock, for phosphate removal from wastewaters, Appl. Clay Sci. 46 (2009) 369–375.
[27] T. Nur, P. Loganathan, T.C. Nguyen, S. Vigneswaran, G. Singh, J. Kandasamy, Batch and column adsorption and desorption of fluoride using hydrous ferric oxide: Solution chemistry and modeling, Chem. Eng. J. 247 (2014) 93–102.
[28] I. Saha, K. Gupta, S. Chakraborty, D. Chatterjee, U.C. Ghosh, Synthesis, characterization and As(III) adsorption behavior of *β*-cyclodextrin modified hydrous ferric oxide, J. Ind. Eng. Chem. 20 (2014) 1741–1751.
[29] D. Tang, Z. Zheng, K. Lin, J. Luan, J. Zhang, Adsorption of *p*-nitrophenol from aqueous solutions onto activated carbon fiber, J. Hazard. Mater. 143 (2007) 49–56.
[30] D. Das, V. Gaur, N. Verma, Removal of volatile organic compound by activated carbon fiber, Carbon 42 (2004) 2949–2962.
[31] Z.J. Qiao, J.J. Li, N.Q. Zhao, N. Wei, Pore size and surface properties of activated carbon fibres modified by high temperature treatment, New Carbon Mater. 19 (2004) 53–56.
[32] J. Liu, Q. Zhou, J. Chen, L. Zhang, N. Chang, Phosphate adsorption on hydroxyl–iron–lanthanum doped activated carbon fiber, Chem. Eng. J. 215–216 (2013) 859–867.
[33] L. Zhang, L. Wan, N. Chang, J. Liu, C. Duan, Q. Zhou, X. Li, X. Wang, Removal of phosphate from water by activated carbon fiber loaded with lanthanum oxide, J. Hazard. Mater. 190 (2011) 848–855.
[34] F.W. Gilcreas, Future of standard methods for the examination of water and wastewater, Health Lab. Sci. 4 (1967) 137–141.
[35] G.-T. Jeong, H.-S. Yang, D.-H. Park, Optimization of transesterification of animal fat ester using response surface methodology, Bioresour. Technol. 100 (2009) 25–30.
[36] K. Mahalik, J.N. Sahu, A.V. Patwardhan, B.C. Meikap, Statistical modelling and optimization of hydrolysis of urea to generate ammonia for flue gas conditioning, J. Hazard. Mater. 182 (2010) 603–610.
[37] J. Zhang, Z. Shen, W. Shan, Z. Mei, W. Wang, Adsorption behavior of phosphate on lanthanum(III)-coordinated diamino-functionalized 3D hybrid mesoporous silicates material, J. Hazard. Mater. 186 (2011) 76–83.
[38] J. Lǔ, H. Liu, R. Liu, X. Zhao, L. Sun, J. Qu, Adsorptive removal of phosphate by a nanostructured Fe–Al–Mn trimetal oxide adsorbent, Powder Technol. 233 (2013) 146–154.
[39] W. Chouyyok, R.J. Wiacek, K. Pattamakomsan, T. Sangvanich, R.M. Grudzien, G.E. Fryxell, W. Yantasee, Phosphate removal by anion binding on functionalized nanoporous sorbents, Environ. Sci. Technol. 44 (2010) 3073–3078.